

# Electron mobility enhancement in strained-germanium *n*-channel metal-oxide-semiconductor field-effect transistors

Y.-J. Yang, W. S. Ho, and C.-F. Huang

Department of Electrical Engineering, National Taiwan University, Taipei, Taiwan 106, Republic of China and Graduate Institute of Electronics Engineering, National Taiwan University, Taipei, Taiwan 106, Republic of China

S. T. Chang

Department of Electrical Engineering, National Chung Hsing University, Taichung, Taiwan 402, Republic of China

C. W. Liu<sup>a)</sup>

Department of Electrical Engineering, National Taiwan University, Taipei, Taiwan 106, Republic of China; Graduate Institute of Electronics Engineering, National Taiwan University, Taipei, Taiwan 106, Republic of China; and National Nano Device Laboratories, Hsinchu, Taiwan 30076, Republic of China

(Received 16 February 2007; accepted 14 August 2007; published online 4 September 2007)

The dependence of electron mobility on strain, channel direction, and substrate orientation is theoretically studied for the germanium *n*-channel metal-oxide-semiconductor field-effect transistors. For the unstrained channel, (111) substrate can provide the highest mobility among the three orientations, mainly due to its largest quantization mass and smallest conductivity mass in *L* valley. The tensile strain parallel to the  $[\bar{1}10]$  channel direction on (111) substrate gives 4.1 times mobility of Si at 1 MV/cm, and the mobility enhancement starts to saturate for the strain larger than 0.5%. The compressive strain of  $\sim 1.5\%$  transverse to  $[\bar{1}10]$  on (111) substrate yields 2.9 times mobility enhancement at 1 MV/cm. © 2007 American Institute of Physics.

[DOI: 10.1063/1.2779845]

Strained-Si technology has been extensively used to improve the performance of advanced Si integrated circuits recently. However, due to the strong demand of high drive current to increase circuit speed, Si is still approaching its physical limits. Ge channel metal-oxide-semiconductor field-effect transistors (MOSFETs) with high mobility attract great interest.<sup>1,2</sup> Although extensive study on strained-Si mobility has been reported,<sup>3-6</sup> not much is known regarding the mobility of Ge under strain. Therefore, we investigate the theoretical limit of Ge mobility under various strain conditions, channel directions, and substrate orientations.

The conduction valley configuration is shown in Fig. 1. In addition to eight half-ellipsoidal *L* valleys, six ellipsoidal  $\Delta$  valleys and one conduction sphere at  $\Gamma$  point are also taken into consideration due to their proximity to *L* valleys in terms of energy. The quantization mass ( $m_z$ ) and the in-plane density-of-state mass ( $m_d$ ) are derived according to Stern and Howard<sup>7</sup> and Rohman *et al.*<sup>8</sup> Note that the mass anisotropy is much stronger for *L* valleys of Ge than  $\Delta$  valleys of Si ( $\sim 20$  for Ge and  $\sim 5$  for Si).

For strained Ge, given the stress magnitude and direction, the strain tensor is obtained using a generalized Hooke's law.<sup>9</sup> The effect of substrate orientation is considered by performing coordinate transformation. The strain-induced band-edge shifts are calculated using the linear deformation-potential theory with the parameters listed in Table I.<sup>10-12</sup> The two-dimensional subband structure is obtained by solving the Poisson and Schrödinger equations self-consistently. The subband energy is a function of un-

strained band gap, strain-induced band-edge shift, and quantization splitting. The momentum relaxation rate is assumed to be isotropic using the relaxation time approximation. The anisotropy of the Ge band structure is retained, and the effective masses are assumed to be unchanged under strain. The Kubo-Greenwood formula<sup>13</sup> is used to calculate the mobility for each subband. The scattering mechanisms take into account intravalley acoustic phonon scattering for each valley, *L-L* intervalley phonon scattering, *L- $\Delta$*  intervalley phonon scattering, and surface roughness scattering. The phonon scattering types and parameters are listed in Table I and are defined in Refs. 14 and 15. Autocorrelation function  $\Delta = 0.4$  nm and correlation length  $l = 1$  nm (Refs. 16 and 17) are used for surface roughness scattering; these are the values of Si, since values of Ge are not known, and a Si passivation layer is sometimes deposited on the Ge channel.<sup>18</sup> The total effective mobility is the population weighted average of all subband mobilities.

The highly anisotropic *L* valley results in unstrained mobility to be significantly dependent on substrate orientation,

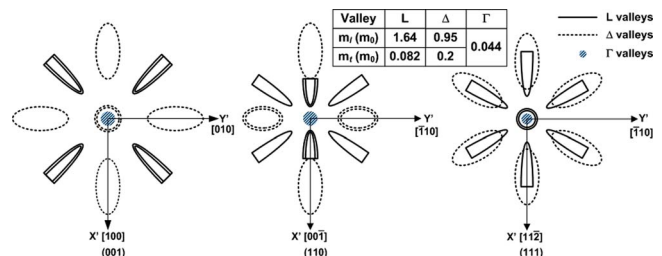


FIG. 1. (Color online) Schematic diagram of the constant-energy contours in the conduction band for various substrate orientations. The inset shows the longitudinal and transverse effective masses of each band (Ref. 8).

<sup>a)</sup> Author to whom correspondence should be addressed; electronic mail: chee@cc.ee.ntu.edu.tw

TABLE I. Bandgap  $E_g$ , dilation deformation potentials  $E_u$  and  $a$ , and shear deformation potential  $E_d$  for  $L$ ,  $\Delta$ , and  $\Gamma$  bands. Also shown are the acoustic deformation potential  $D_{ac}$  for intervalley phonon scattering, and the deformation potential  $\Theta$  and  $D_iK$  for intervalley phonon scattering.

Band	$L$	$\Delta$	$\Gamma$
Bandgap $E_g$ (eV)	0.66	0.85	0.8
$E_u$ (eV)	16.8	9.75	
$E_d + E_u/3 - a$ (eV)	-0.83	5.75	
$a$ (eV)	2	2	-8.97
$D_{ac}$ (eV)	13.5	9	5
Type of intervalley phonon scattering	$\Theta$ (K)	$D_iK$ ( $10^8$ eV/cm)	
$LL_1$ (LA, LO)	320	3.0	
$LL_2$ (TA)	120	0.2	
$L\Delta$ (LA)	320	4.1	

i.e.,  $\text{Ge}(111) > \text{Ge}(110)[\bar{1}10] > \text{Ge}(001) > \text{Ge}(110)[00\bar{1}]$ . ( ) and [ ] are the notations of substrate orientation and channel direction, respectively. Regarding the in-plane mobility anisotropy in unstrained channels, only (110) substrate shows anisotropy for different channel directions due to the twofold symmetry of the valley configuration (Fig. 1). In the case of unstrained (111) substrate, most electrons occupy the central  $L$  valleys (Fig. 1) due to its relatively large quantization mass, and the smallest conductivity effective mass of the central  $L$  valleys leads to the highest mobility.

In general, the mobility under uniaxial strain is channel-direction dependent. The channel directions to achieve the highest mobility on (111), (110), and (001) substrates occur at  $[\bar{1}10]$ ,  $[\bar{1}\bar{1}0]$ , and  $[110]$ , respectively, with the tensile stress of 1 GPa ( $\sim 0.7\%$  strain) parallel to the channel direction (Fig. 2).<sup>5</sup> The enhancement is mainly attributed to the reduction of average conductivity mass caused by the electron repopulation from valleys with large conductivity mass to those with small conductivity mass. To ensure the validity of our approach, the calculated mobility of Si (001) is compared with the published data<sup>19</sup> (Fig. 2) and reasonable agreement is achieved.

Figure 3 shows mobility as a function of biaxial strain on (001) substrate. For strain smaller than 0.7% ( $\sim 1$  GPa),  $L$  valleys dominate the mobility due to its occupancy exceeding 70%. Thus, the mobility under small biaxial strain is

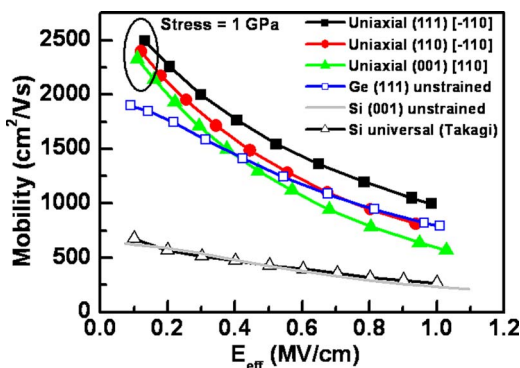


FIG. 2. (Color online) Mobility as a function of effective vertical field for the uniaxial tensile stress of 1 GPa parallel to the channel direction on different substrate orientations. The mobility of unstrained Ge(111) channel and the Si universal mobility curve (Ref. 19) are also shown for comparison.

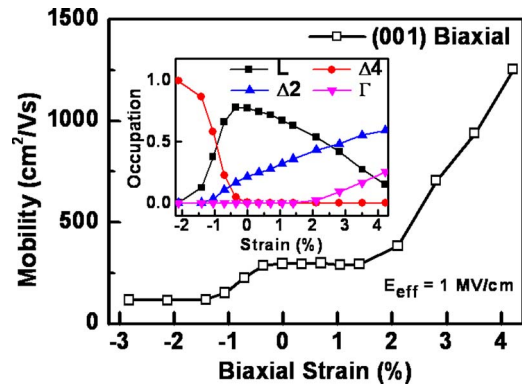


FIG. 3. (Color online) Mobility as a function of biaxial strain for (001) substrate at  $E_{\text{eff}} = 1$  MV/cm. The inset shows the corresponding valley occupation vs strain.

similar to the unstrained case. In the case of the tensile strain larger than 2% ( $\sim 2.8$  GPa), the mobility increases rapidly. Significant occupancy in light-mass  $\Gamma$  band for tensile strain larger than 2% is responsible for this (Fig. 3). However, the mobility enhancement for Ge channel on (001) substrate under large biaxial tensile strain is not as high as that in the bulk case, which has no quantum confinement and yields mobility over  $10\,000$   $\text{cm}^2/\text{V s}$  at 2% biaxial tensile strain.<sup>10</sup> This is due to the quantum confinement at high vertical field, which leads to less occupancy of  $\Gamma$  band in Ge channel than that of bulk Ge. On the other hand,  $\Delta_4$  valleys dominate the occupancy when compressive strain is larger than 1%, and the mobility is degraded due to the larger mass in  $\Delta_4$  valleys than that in  $L$  valleys.

Mobility as a function of strain for (111) $[\bar{1}10]$ , (110) $[\bar{1}\bar{1}0]$ , and (001) $[110]$  at 1 MV/cm is shown in Fig. 4. Note that biaxial strain is independent of the stress direction, while uniaxial tensile and compressive stress are applied parallel and perpendicular to the channel direction, respectively, as shown in Fig. 4. The perpendicular tensile strain has lower mobility than the parallel tensile strain, and the mobility under the parallel compressive strain is inferior to the perpendicular compressive strain. Therefore, these data are not shown in Fig. 4. Under large strain, electrons are all populated in the valleys with the lowest energy, and the average conductivity mass remains constant. Therefore, the mobility remains constant at large strain. Biaxial tensile strain and longitudinal tensile strain along the  $[\bar{1}10]$  channel direction

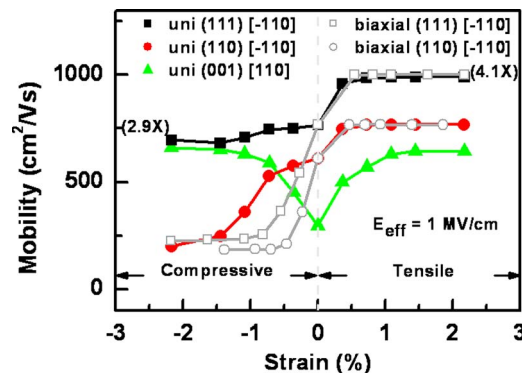


FIG. 4. (Color online) Mobility as a function of strain under different stress conditions, channel directions with notation of [ ], and substrate orientations with notation of ( ).

give similar mobility enhancement on (111) substrate. For (111)[ $\bar{1}10$ ], the highest mobility enhancement of 4.1 times of Si(001) universal mobility is achieved when tensile strain is larger than 0.5% ( $\sim 0.7$  GPa). For transverse compressive strain larger than 1.5% ( $\sim 2.1$  GPa), the mobility enhancement is found to be 2.9 times of Si(001) universal mobility. However, the mobility decreases very rapidly under biaxial compressive strain and falls below the Si universal mobility (Fig. 2) for (110) and (111) substrates. The band edges of  $L$  valleys and  $\Delta$  valleys become close under biaxial compressive strain, and the scattering rate increases accordingly. Both increases of conductivity effective mass and scattering rate account for the mobility degradation under compressive biaxial strain.

The strain effect on electron mobility of Ge  $n$ -MOSFETs is investigated. The (111) Ge FETs have the highest mobility among all three substrate orientations. The mobility enhancement can be found for all three substrate orientations if the channel direction and strain condition are optimized. The mobility optimization can facilitate the device design of Ge channel MOSFETs.

The National Taiwan University group is supported by National Science Council, Taiwan, under Contract No. NSC 95-2221-E-002-357. The grant from TSMC (Taiwan Semiconductor Manufacturing Company) is highly appreciated.

- <sup>1</sup>C. C. Yeo, B. J. Cho, F. Gao, S. J. Lee, M. H. Lee, C.-Y. Yu, C. W. Liu, L. J. Tang, and T. W. Lee, *IEEE Electron Device Lett.* **26**, 761 (2005).
- <sup>2</sup>M. L. Lee and E. A. Fitzgerald, *Appl. Phys. Lett.* **83**, 4202 (2003).
- <sup>3</sup>S. Maikap, C.-Y. Yu, S.-R. Jan, M. H. Lee, and C. W. Liu, *IEEE Electron Device Lett.* **25**, 40 (2004).
- <sup>4</sup>S. Dhar, H. Kosina, V. Palankovski, S. E. Ungersboeck, and S. Selberherr, *IEEE Trans. Electron Devices* **52**, 527 (2005).
- <sup>5</sup>H. Irie, K. Kita, K. Kyuno, and A. Toriumi, *Tech. Dig. - Int. Electron Devices Meet.* **2004**, 225.
- <sup>6</sup>K. Uchida, T. Krishnamohan, K. C. Saraswat, and Y. Nishi, *Tech. Dig. - Int. Electron Devices Meet.* **2005**, 129.
- <sup>7</sup>F. Stern and W. E. Howard, *Phys. Rev.* **163**, 816 (1967).
- <sup>8</sup>A. Rahman, M. S. Lundstrom, and A. W. Ghosh, *J. Appl. Phys.* **97**, 053702 (2005).
- <sup>9</sup>J. J. Wortman and R. A. Evans, *J. Appl. Phys.* **36**, 153 (1965).
- <sup>10</sup>I. Balslev, *Phys. Rev.* **143**, 636 (1966).
- <sup>11</sup>M. V. Fischetti and S. E. Laux, *J. Appl. Phys.* **80**, 2234 (1996).
- <sup>12</sup>J. Liu, D. D. Cannon, K. Wada, Y. Ishikawa, D. T. Danielson, S. Jongthammanurak, J. Michel, and L. C. Kimerling, *Phys. Rev. B* **70**, 155309 (2004).
- <sup>13</sup>R. Kotlyar, D. Giles, P. Matagne, B. Obradovic, L. Shifren, M. Stettler, and E. Wang, *Tech. Dig. - Int. Electron Devices Meet.* **2004**, 391.
- <sup>14</sup>S. Takagi, J. L. Hoyt, J. J. Welser, and J. F. Gibbons, *J. Appl. Phys.* **80**, 1567 (1996).
- <sup>15</sup>C. Jacoboni and L. Reggiani, *Rev. Mod. Phys.* **55**, 645 (1983).
- <sup>16</sup>T. Low, M. F. Li, C. Shen, Y.-C. Yeo, Y. T. Hou, and C. Zhu, *Appl. Phys. Lett.* **85**, 2402 (2004).
- <sup>17</sup>B. Ghosh, X. Wang, X.-F. Fan, L. F. Register, and S. K. Banerjee, *IEEE Trans. Electron Devices* **52**, 547 (2005).
- <sup>18</sup>C.-Y. Peng, F. Yuan, C.-Y. Yu, P.-S. Kuo, M. H. Lee, S. Maikap, C.-H. Hsu, and C. W. Liu, *Appl. Phys. Lett.* **90**, 012114 (2007).
- <sup>19</sup>S. Takagi, A. Toriumi, M. Iwase, and H. Tango, *IEEE Trans. Electron Devices* **41**, 2357 (1994).